Biochimica et Biophysica Acta 1818 (2012) 2158–2170

Contents lists available at SciVerse ScienceDirect

Biochimica et Biophysica Acta

journal homepage: www.elsevier.com/locate/bbamem

Structural and thermodynamic insight into the process of "weak" dimerization of the ErbB4 transmembrane domain by solution NMR

Eduard V. Bocharov [a,*,1], Konstantin S. Mineev [a,1], Marina V. Goncharuk [a,b], Alexander S. Arseniev [a]

[a] Shemyakin-Ovchinnikov Institute of Bioorganic Chemistry RAS, str. Miklukho-Maklaya 16/10, Moscow, 117997 Russian Federation
[b] Lomonosov Moscow State University, Moscow, 119991, Russian Federation

ARTICLE INFO

Article history:
Received 3 December 2011
Received in revised form 20 April 2012
Accepted 1 May 2012
Available online 8 May 2012

Keywords:
Receptor tyrosine kinase
Transmembrane domain
Dimerization
Spatial structure
Thermodynamics
NMR

ABSTRACT

Specific helix–helix interactions between the single-span transmembrane domains of receptor tyrosine kinases are believed to be important for their lateral dimerization and signal transduction. Establishing structure–function relationships requires precise structural-dynamic information about this class of biologically significant bitopic membrane proteins. ErbB4 is a ubiquitously expressed member of the HER/ErbB family of growth factor receptor tyrosine kinases that is essential for the normal development of various adult and fetal human tissues and plays a role in the pathobiology of the organism. The dimerization of the ErbB4 transmembrane domain in membrane-mimicking lipid bicelles was investigated by solution NMR. In a bicellar DMPC/DHPC environment, the ErbB4 membrane-spanning α-helices $(651–678)_2$ form a right-handed parallel dimer through the N-terminal double GG4-like motif $A^{655}GxxGG^{660}$ in a fashion that is believed to permit proper kinase domain activation. During helix association, the dimer subunits undergo a structural adjustment (slight bending) with the formation of a network of inter-monomeric polar contacts. The quantitative analysis of the observed monomer–dimer equilibrium provides insights into the kinetics and thermodynamics of the folding process of the helical transmembrane domain in the model environment that may be directly relevant to the process that occurs in biological membranes. The lipid bicelles occupied by a single ErbB4 transmembrane domain behave as a true ("ideal") solvent for the peptide, while multiply occupied bicelles are more similar to the ordered lipid microdomains of cellular membranes and appear to provide substantial entropic enhancement of the weak helix–helix interactions, which may be critical for membrane protein activity.

1. Introduction

Despite their involvement in a large variety of processes in living organisms, membrane proteins are a challenging subject for modern structural biology and are still poorly explored. Most membrane proteins are composed of a number of transmembrane (TM) α-helices, which interact with each other and thus form a tertiary structure inside the lipid bilayer. The folding of helical segments into a TM domain as well as the functional mobility of certain helices often determine the functional characteristics of the full-size membrane protein. Thus, it is necessary to study the principles underlying TM helix–helix interactions.

Bitopic proteins, which have only a single α-helical TM domain separating the ecto- and cytoplasmic domains, are a class of biologically significant membrane proteins that provide a convenient means to study helix–helix interactions in the membrane. The regulation of the activity of these proteins is mostly associated with their lateral dimerization in cell membranes. Homo- and heterodimerization of bitopic proteins was once thought to primarily involve extracellular and cytoplasmic domains, but recent studies have made it increasingly clear that the TM domains are also critical for dimerization and modulate the biological function of the proteins [1,2]. Furthermore, some polymorphisms and mutations in the TM domains of bitopic proteins have been implicated in numerous human diseases [3]. Upon bitopic protein activation, which can be ligand-dependent or -independent, significant intra-molecular conformational transitions result in the rearrangement of the receptor domains and subsequent receptor dimerization or switching from one dimerization state to another, e.g., a ligand-dependent transition from the preformed inactive dimeric state to the active dimer, as has been proposed for the ErbB receptor tyrosine kinases [4–8].

Proteins from the epidermal growth factor receptor family, also known as HER or ErbB, which transmit biochemical signals across the plasma membrane, play an important role in cell growth and differentiation events in embryonic and adult tissues, whereas inappropriate ErbB activity is implicated in human diseases, including several cancers [9,10]. The single-span α-helical TM domains of ErbB can

Abbreviations: ErbB, epidermal growth factor receptor; TM, transmembrane; NOE, nuclear Overhauser effect; NOESY, NOE spectroscopy; MHP, molecular hydrophobicity potential; DMPC, dimyristoylphosphatidylcholine; DHPC, dihexanoylphosphatidylcholine

* Corresponding author at: Str. Mikluho-Maklaya, 16/10, Moscow, 117997 Russian Federation. Tel.: +7 495 330 74 83.
E-mail address: bon@nmr.ru (E.V. Bocharov).

[1] Eduard V. Bocharov and Konstantin S. Mineev contributed equally to this work.

0005-2736/$ – see front matter © 2012 Elsevier B.V. All rights reserved.
doi:10.1016/j.bbamem.2012.05.001

homo- and heterodimerize in the absence of the extracellular ligand-binding and cytoplasmic kinase domains [5,11]. Mutagenesis studies have shown that the ErbB TM domains interact through the so-called GG4 motifs [5,12,13], a small-X_3-small tetrad repeat of small side chain-containing residues separated by three other residues [14]. The TM segments of all four human ErbB receptors have at least one such motif, and all except ErbB3 have two motifs, which are located in the N- and C-terminal portions of the TM helices. The ErbB3 TM domain can also self-associate through a non-standard heptad repeat motif [15]. The switching of helices between two possible conformations of the dimeric TM domain is thought to be one of the key stages of ErbB signal transduction [5-8]. The measured dissociation constants of various TM helical homo- and heterodimers formed by different members of the ErbB family have permitted the establishment of the structure–energy relationship for "weak" TM helix–helix associations [11,16].

ErbB4 is a ubiquitously expressed member of the HER/ErbB family of receptor tyrosine kinases, which are essential for normal development of different adult and fetal human tissues [17]. Neuregulins and certain ligands of the EGF family, which trigger the activation of the ErbB4 receptor and subsequent signaling, induce a spectrum of cellular responses such as mitogenesis, differentiation, growth inhibition, and survival [17]. The ligand-induced translocation of ErbB4 and associated signaling molecules into lipid rafts is critical for signal transduction [18]. Additionally, ErbB4 is a unique member of the ErbB family because its TM domain undergoes proteolytic processing by the presenilin-dependent γ-secretase within the cell membrane to release the intracellular domain, a critical event that regulates multiple receptor signaling activities, including proapoptotic activity [19]. Recent clinical studies have revealed that tumoral expression of ErbB4 improves the overall survival of breast cancer patients, and thus ErbB4 signaling is believed to play a significant role in cancer pathobiology [20,21]. Therefore, a structural-thermodynamic investigation of the dimerization process of the ErbB4 TM domain would aid in the elucidation of the underlying mechanisms of TM helix–helix association and signal transduction and provide a basis for the molecular design of pharmaceutical compounds that affect the specific helix–helix interaction in the cell membrane for the appropriate control of receptor kinase activity. In the present work, we have studied the self-association of the ErbB4 TM domain; solution NMR spectroscopy was used to obtain its homodimeric spatial structure and describe the monomer–dimer transition under experimental conditions in membrane-mimicking lipid bicelles. The processes observed during homodimer formation reveal some aspects of the kinetics and thermodynamics of helix–helix association that may be relevant to the process that occurs in biological membranes, providing a better understanding of membrane protein function.

2. Material and methods

2.1. NMR sample preparation

The recombinant isotopically labeled TM fragment $ErbB4_{642–685}$, ErbB4tm, was produced in bacteria and purified as described in Ref. [22]. Three ErbB4tm samples were prepared: uniformly ^{15}N-labeled, $^{15}N,^{13}C$-labeled, and a 1:1 mixture of uniformly $^{15}N,^{13}C$-labeled and unlabeled proteins ("isotopic-heterodimer" sample). The ErbB4tm samples were incorporated into small dimyristoylphosphatidylcholine/dihexanoylphosphatidylcholine (DMPC/DHPC) lipid bicelles with an effective lipid/protein molar ratio (L/P) of 35 to 230 at a total lipid concentration of 50 or 110 mM in a buffer solution containing 20 mM deuterated sodium acetate, 0.15 μM sodium azide, 1 mM EDTA, and 5% D_2O or 99.9% D_2O (v/v), pH 5.0. The effective molar ratio q of long- and short-chain lipids in the bicelle was 0.27, assuming a free DHPC concentration of 7 mM in the bicellar suspension [23]. Unless otherwise specified, lipids with deuterated hydrophobic tails were used. Deuterated 1,2-di-[$^2H_{27}$]-myristoyl-*sn*-glycero-3-phosphocholine (d_{54}-DMPC) and 1,2-di-[$^2H_{11}$]-myristoyl-*sn*-glycero-3-phosphocholine (d_{22}-DHPC) were synthesized from *sn*-glycero-3-phosphocholine by acylation with anhydrides of d_{27}-myristic acid and d_{11}-hexanoic acid, respectively, as described in [24].

First, ErbB4tm was dissolved in 1:1 water/trifluoroethanol at room temperature, supplemented with DMPC/DHPC (also in water/trifluoroethanol mixture), lyophilized and dissolved in the water buffer. Before NMR studies, the samples were subjected to several freeze/thaw cycles to ensure a uniform protein distribution among the lipid bicelles. An Eppendorf vial containing the NMR sample was frozen in a liquid nitrogen bath and kept at room temperature for ~10 min. The 5 freeze/thaw cycles were usually performed with slightly sonication of the samples at each cycle to obtain a clear solution and good NMR spectra. To verify the validity of experimental conditions, circular dichroism (JASCO-810 spectropolarimeter, Jasco, Tokyo, Japan) measurements were performed. The circular dichroism spectra were virtually identical for ErbB4tm incorporated into DMPC/DHPC bicelles and DMPC unilamellar liposomes, revealing approximately 62% α-helical structure in both cases.

2.2. NMR chemical shift assignments and structure determination

NMR spectra were acquired at 313 K on a 700-MHz Avance spectrometer (Bruker BioSpin, Rheinstetten, Germany) equipped with a pulsed-field gradient triple-resonance cryoprobe. The ^1H, ^{13}C, and ^{15}N resonances of ErbB4tm were assigned with CARA software [25] with triple-resonance techniques [26,27] as described in Appendix A: Supplementary data, Section A.1.

The local effective rotation correlation times (τ_R) for the individual ^{15}NH groups of ErbB4tm were calculated with DASHA software [28] from the ratio of the ^{15}N longitudinal and transverse relaxation times obtained at L/P ≈ 120 as described in Ref. [29].

The spatial NMR structure of the ErbB4tm homodimer was calculated with the CYANA program [30] based on intra- and inter-monomeric NOE distance restraints derived from the analysis of three-dimensional ^{15}N- and ^{13}C-edited NOESY and $^{15}N,^{13}C$-F1-filtered/F3-edited-NOESY spectra [26,31] acquired for the ^{15}N- and $^{15}N,^{13}C$-labeled ErbB4tm and $^{15}N,^{13}C$-ErbB4tm/ErbB4tm "isotopic-heterodimer" samples (at L/P ≈ 50). The backbone dihedral angle restraints for φ and ψ were estimated basing on the assigned chemical shifts with the program PREDITOR [32]. The spatial structure calculation procedure is described in Appendix A: Supplementary data, Section A.1.

The hydrophobic properties of the α-helices in the ErbB4tm dimer were calculated with the molecular hydrophobicity potential (MHP) approach [33] as described in Appendix A: Supplementary data, Section A.2. The contact area between the dimer subunits was calculated with the DSSP program [34] as the difference between the accessible surface areas of ErbB4tm residues in the monomer and dimer. The ErbB4tm dimer structures were visualized with the MOLMOL program [35].

2.3. NMR measurements of kinetics and thermodynamics

The dependence of the dimer association constants of ErbB4tm on the lipid concentration was treated according to the protein–bicelle complex model (similar to the protein–micelle model proposed in [36–39]), assuming that the apparent free energy of association:

$$\Delta G_{app} = \Delta G_0 + \gamma RT \ln[Lip]_B, \quad (1)$$

where ΔG_0 is the standard free energy of association, γ is a measure of the ideality of a bicellar system (formally the reaction order on the lipid) [15,38], R is the universal gas constant, T is the temperature in K, and $[Lip]_B$ is the concentration of the lipid in bicellar form, which corresponds to the overall lipid concentration excluding the free

lipid concentration that is usually estimated to be equal to the critical micelle concentration (CMC).

The apparent free energy of association is related to the classic association constant for bimolecular interactions ($K_{app} = D/M^2$):

$$\Delta G_{app} = -RT\ln\left(K_{app}\right) = RT\ln\left(M^2/D\right), \quad (2)$$

where M and D are the concentrations of the monomeric and dimeric protein, respectively.

Eqs. (1) and (2) may be rewritten in the form:

$$K_A = e^{\frac{-\Delta G_0}{RT}} = {}^{D[Lip]_B^{\gamma}}\!/_{M^2}, \quad (3)$$

where K_A is the constant of the association, taking into account the lipid-related processes.

When $\gamma = 1$, the solvent is true (sometimes referred to as "ideal") [38], and ΔG_0 can be directly derived from the reduced association constant (K_{AR}):

$$K_{AR} = K_{app}[Lip]_B = {}^{D[Lip]_B}\!/_{M^2}, \quad (4)$$

which is K_{app} written for the concentration of protein measured relative to lipid concentration. When γ is other than unity, ΔG_0 is the parameter of the system and cannot be compared to that of another protein except when its dimerization is described by an identical γ parameter [15,38]. If the lipid is not an "ideal" solvent but acts as a reactant, its quantity in the bicelle is believed to change upon the association of TM helices, and $(\gamma - 1)$ would formally indicate the average number of lipid molecules leaving ($(\gamma - 1) > 0$) or entering ($(\gamma - 1) < 0$) the system after dimer formation [15,36–39]. However, variations in γ can also imply that the constant of the reaction depends on some factor other than the alteration of amounts of lipid molecules in a supramolecular system.

To measure ΔG_0, a ^{15}N-labeled ErbB4tm sample with an initial L/P ratio of 80 at 40 mM total lipid concentration was titrated by adding small portions of a concentrated bicelle suspension to a final L/P ratio of 230 at 100 mM total lipid concentration while maintaining the protein concentration near 0.52 ± 0.05 mM. The sample underwent several freeze/thaw cycles at each L/P point. The monomer/dimer ratio was calculated from the integrals of the corresponding cross-peaks in ^{1}H/^{15}N TROSY spectra and was used to determine the monomer (M) and dimer (D) concentrations. The cross-peaks of the amide group of G^{656} corresponding to the monomer and dimer states of ErbB4tm were used for the calculation because they do not overlap with other peaks. The projections of the 2D cross-peaks of the two states of G^{656} were fitted by Lorentzian lines in Mathematica software. The resulting lines were integrated and scaled with respect to the proton transverse relaxation during the INEPT transfers in the ^{1}H/^{15}N TROSY pulse sequence. The nitrogen transverse relaxation was neglected. At each L/P ratio, the reduced association constant K_{AR} and corresponding ΔG_{app} were calculated. The dependence of ΔG_{app} on $\ln[Lip]_B$ was fitted to Eq. (1) at L/P > 120, when the bicelle unambiguously contained, on average, less than one protein (given a bicelle size of ~100 lipids and a free DHPC concentration of 7 mM [23,40]). The temperature dependence of ΔG_{app} was determined similarly.

The temperature dependence of the apparent free energy of ErbB4tm association was investigated at two L/P ratios of 50 and 80 at a total lipid bicellar concentration of 93 mM at a temperature range of 288–323 K. Under both conditions, the curves describing the temperature dependence of the free energy appeared to be strongly nonlinear, suggesting that the complex model should be employed for data analysis. A rather good fit was obtained with the relationship [41]:

$$\Delta G(T) = \Delta H_0 - T\Delta S_0 + \Delta C_p(T - T_0) - T\Delta C_p \ln\left({}^{T}\!/_{T_0}\right), \quad (5)$$

where ΔH_0 and ΔS_0 are the standard enthalpy and entropy of dimerization and ΔC_p is the change of the heat capacity upon dimerization at the standard-state reference temperature T_0 (298 K in this study). The more complex formalism, which includes the temperature dependence of ΔC_p, was not applied because the acquired data matched the above written formula within the limits of the experimental errors under both conditions.

To monitor the temperature dependence of the hydrodynamic radius of the DMPC/DHPC bicelle with embedded ErbB4tm (at L/P ≈ 50), the translational diffusion of the lipids and ErbB4tm was measured from ^{1}H-DOSY spectra [27] acquired at a temperature range of 288–323 K (at pH 5.0).

The kinetic rate constants for dissociation and dimerization of ErbB4tm were measured from the intensities of the exchange and diagonal cross-peaks in ^{15}N-edited NOESY spectra recorded with a 100-ms mixing time according to the equations [42]:

$$\begin{aligned} I_M &= p_M[p_M + p_D\exp\{-k_{ex}\tau\}]\exp[-R_1\tau] \\ I_D &= p_D[p_D + p_M\exp\{-k_{ex}\tau\}]\exp[-R_1\tau] \\ I_{DM} &= I_{MD} = p_M p_D[1 - \exp\{-k_{ex}\tau\}]\exp[-R_1\tau] \end{aligned} \quad (6)$$

where I_M, I_D, I_{DM} and I_{MD} are the intensities of the diagonal peaks for the monomeric (M) and dimeric (D) states and of the cross-peaks between them, p_D and p_M are the populations of the two states, τ is the mixing time, R_1 is the rate of proton longitudinal relaxation, and k_{ex} is the exchange rate:

$$k_{ex} = k_{diss} + \tilde{k}_{dim} = k_{diss} + k_{dim}M/[Lip]_B, \quad (7)$$

where k_{diss} is a first-order rate constant of dissociation, k_{dim} is a second-order rate constant of dimerization, and $\tilde{k}_{dim}$ is a generalized dimerization rate constant ($\tilde{k}_{dim} = k_{dim}M/[Lip]_B$). The rate constants can be extracted, taking into account the equilibrium population of the states and knowing that $p_M + 2p_D = 1$ and $\frac{k_{diss}}{k_{dim}} = \frac{p_M^2(M+2D)}{p_D[Lip]_B}$, where $(M + 2D)$ is the total protein concentration.

Dimerization rate constants were also measured by line shape analysis. The ^{1}H/^{15}N TROSY spectra of ErbB4tm samples for the monomer (at the L/P ratio of 120) and monomer/dimer mixture (at the L/P ratio of 50) were acquired at different temperatures. The ^{1}H projections of the 2D cross-peaks of G^{656} in the pure monomeric state and in two states in the monomer/dimer mixture were fitted by Lorentzian lines with Mathematica software (Wolfram Research, U.S.A.). The ^{1}H linewidth measured for the pure monomer was subtracted from the linewidth of the monomer in the monomer/dimer mixture, and the result was multiplied by π to give the generalized dimerization rate constant $\tilde{k}_{dim}$. The foregoing assumes that the exchange was slow (on the NMR chemical shift timescale [42]) at temperatures below 313 K. Generalized rate constants were used to calculate dimerization rate constants; the monomer and dimer concentrations were obtained by the lineshape fitting performed to determine the magnitude of ΔG_0. The resulting rate constants were fitted to the simple Arrhenius equation ($k = A\exp(-E_a/RT)$) or used to calculate the free energy of the transition state. The relative free energies $\Delta G_A^{\ddagger}$ and $\Delta G_D^{\ddagger}$ of the transition state accompanying the association and dissociation of ErbB4tm were estimated from the obtained rate constants according to the Eyring equation [43]:

$$\begin{aligned} \Delta G_A^{\ddagger} &= RT\ln(k_B T\kappa/hk_{dim}), \\ \Delta G_D^{\ddagger} &= RT\ln(k_B T\kappa/hk_{diss}), \end{aligned} \quad (8)$$

where k_B and h are the Boltzmann and Planck's constants, respectively, and κ is the transmission coefficient, which is related to the fraction of molecules in the transition state that end up as products. A value of $\kappa \approx 1.6 \times 10^{-7}$ was previously estimated for globular protein folding [44].

3. Results and discussion

3.1. The ErbB4 transmembrane domain undergoes a slow monomer–dimer transition in the bicellar environment

To investigate the structural and dynamic behavior of the TM domain of the ErbB4 receptor tyrosine kinase, we prepared a recombinant 44-residue fragment ErbB4$_{642-685}$ (named ErbB4tm), which includes residues STLPQHARTPLIAAGVIGGLFILVIVGLTFAVYVRRKSIKKKRA and contains the proposed hydrophobic TM segment (underlined residues 652–675; the sequence numbering corresponds to the Swiss-Prot annotation of the human receptor, Q15303). The hydrophobic nature of the membrane-spanning ErbB4tm requires a membrane-mimicking environment in the form of supramolecular particles that tumble fast enough to give well-resolved resonance lines when solution NMR methods are used. We recently resolved the dimeric structures of TM domains of human proteins, including the ErbB receptor family, and concluded that discoidal mixed bicelles (a small circular bilayer of long-chain lipids surrounded by a rim of short-chain lipids) are a fairly adequate model of lipid membranes for structural studies by high-resolution NMR [45–49]. Therefore, ErbB4tm was dissolved in DMPC/DHPC bicelles with an effective molar ratio of long- and short-chain lipids $q \approx 0.27$ (adjusted for the free DHPC concentration in the bicellar suspension [23]).

^{15}N and ^{13}C isotope-labeled ErbB4tm embedded into bicelles with a lipid/protein molar ratio (L/P) and total lipid concentration varying from 35 to 230 and 50 mM to 110 mM, respectively, was investigated with conventional heteronuclear NMR in the temperature range of 288–328 K at pH 5.0. Under the specified conditions, two sets of signals with different peak intensities are observed in the NMR spectra (Fig. 1) of the N-terminal portion of the TM α-helical region 650–677 of ErbB4tm (see Appendix A: Supplementary data, Section A.3 and Fig. A.1). At low temperatures, the exchange between the two states is slow on the NMR chemical shift timescale (Fig. 1). Because the minimal distinguishable chemical shift difference between the signals for the two states was ~20 Hz at 288 K (23 Hz for $\Delta\delta(^{15}N^{H})$ of G^{660}), we can estimate that the exchange rate is slower than 20 s^{-1}. At temperatures above 323 K, the two sets merge into one with average peak positions that indicate that the slow exchange process becomes fast on the NMR timescale (Fig. 1). The cross-peaks in the ^{15}N/^{13}C-filtered NOESY spectra [31], which denote inter-molecular interactions in the ErbB4tm "isotopic-heterodimer" sample, vanish gradually with the simultaneous increase in the first-state population, which becomes abundant at high L/P values. The second state dominates in bicelles saturated with protein, but as the L/P ratio decreases to 35, the samples become unstable with the formation of ~20 nm (according to light scattering measurements, unpublished data) aggregates within three days. At L/P values near 50, when the populations of both states are equal and the sample is rather stable, the eight unambiguous inter-monomeric NOE contacts are detected between the methyl groups (which have the smallest relaxation rates) of the ^{13}C,^{15}N-labeled ErbB4tm and the other groups of the unlabeled ErbB4tm (Table A.1 and Fig. A.2), directly demonstrating that the protein self-associates in a dimer with parallel orientation. Thus, the observed process is a slow monomer–dimer transition (millisecond timescale), in which the populations of states and, consequently, apparent dissociation constants are dependent on the L/P ratio (Fig. 1B), which is related to the effective concentration of the protein in the bicelle. The presence of distinct signals for the monomeric and dimeric states and the directly measured inter-monomeric NOE connectivities unambiguously demonstrate that the dimerization of ErbB4tm is specific and eliminates the need for experiments used in recent works [50] to confirm the specific character of the TM helix–helix interaction when the dimer–monomer transition is fast.

3.2. Spatial structure of the homodimeric ErbB4 transmembrane domain

Only one set of signals can be observed in the ^{1}H/^{15}N HSQC spectra for ErbB4tm in the dimeric state, indicating that its structure is symmetrical on the NMR timescale (Fig. 1B). Therefore, the intra- and inter-monomeric NOE restraints identified in NMR spectra of ErbB4tm as well as torsion angle restraints derived from the chemical shifts were symmetrized to provide proper dimer spatial structure. An overview of the input data, statistics and parameters of the calculated set of spatial structures is presented in Table 1. The atomic coordinates and experimental restraints for the ensemble of 20 structures of the ErbB4tm dimer embedded into the DMPC/DHPC bicelles has been deposited in the Protein Data Bank under accession code PDB ID: 2LCX (Fig. A.3). Under experimental conditions, the ErbB4 TM domain represents a parallel, symmetric dimer of membrane-spanning α-helices, residues 651–678, with the axes of the helices oriented at an angle θ of −40° and a distance d of 7.2 Å (Fig. 2A).

According to the spatial distribution of the hydrophilic/hydrophobic properties of the ErbB4tm dimer subunits, which were visualized by molecular hydrophobicity potential (MHP) [33], the helix-packing interface, which extends over 360 Å^2 (per subunit), is rather polar, with some hydrophobic segments on the outer surface (Fig. 2B). So, the self-association of the ErbB4tm α-helix is driven by polar interactions through the N-terminal double GG4-like motif A^{655}GxxGG^{660}; residues P^{651}, L^{652}, I^{663}, L^{664} and V^{667} assist by stabilizing the structure of the dimer by forming close van der Waals contacts between their bulky side chains. On the C-terminal flank of the helix-packing interface, the aromatic rings of opposite F^{671} residues participate in an intermolecular edge-face stacking interaction. At the adjacent side of the TM helix, the side chain hydroxyl group of T^{670} participates in intramolecular hydrogen bonding with the carbonyl group of I^{666}, which supports the local structure of the helix. The other weakly polar surface of the ErbB4tm helix, which includes the unused C-terminal GG4-like motif G^{668}xxxA^{672}, is facing lipids. This surface may be used for switching between the active and inactive receptor states, which are presumably associated with the dimerization of the TM domain *via* the N- and C-terminal motifs, as was suggested for the ErbB family in the "rotation coupling" activation mechanism [5–7].

Recently, it was proposed that interactions between α-helices in the lipid bilayer are partially mediated by polar interactions between Hα hydrogens and carbonyl groups that have properties similar to those of hydrogen bonds but lower energies [53–55]. Three symmetrical contacts (6 per dimer) of this type occur in the NMR-derived structure set of the ErbB4tm dimer: CαH$_1$ of G^{656}, CαH$_2$ of G^{659}, and CαH$_1$ of G^{660} interact with the opposite backbone carbonyls of A^{655}, G^{656}, and G^{659}, respectively (Fig. 2C). However, unlike the strong homodimerization of the GpA TM domain, which is also mediated by the GG4-like motif [56], a strong downfield shift of the ^{1}Hα1/^{1}Hα2 glycine resonances (up to 0.7 ppm for GpA) for the suggested donors of non-canonical hydrogen bonds is not observed, and the maximal downfield shift registered for G^{656} is 0.22 ppm. Thus, the interhelical contacts in the determined ErbB4tm dimer structure are apparently not hydrogen bonds but weak electrostatic interactions between partial charges. This is in agreement with the weaker dimerization of the ErbB TM domains in comparison with the GpA TM self-association, which is seemingly typical for RTKs [11,57–59].

It has been proposed that kinase domain activation requires the folding of the cytoplasmic juxtamembrane regions of both monomers in the ErbB dimer into an antiparallel helical structure in which the spacing between the C-termini of the TM helices is approximately 2 nm [51]. The determined structure of the homodimer formed *via* the N-terminal double GG4-like motif of the ErbB4 TM domain

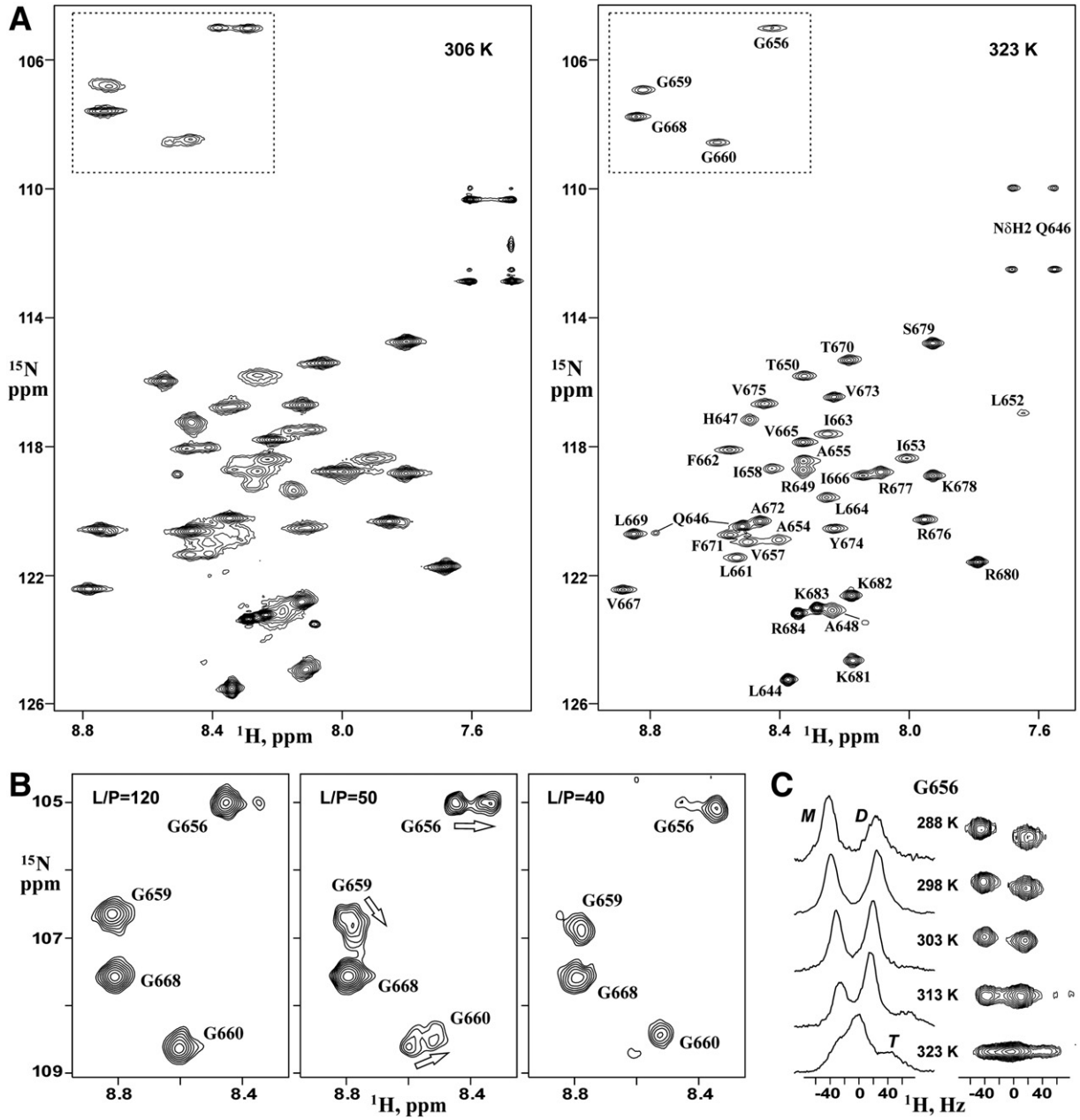

Fig. 1. ErbB4tm monomer–dimer equilibrium characterized by peak doubling in the NMR spectra. (A) The ^{1}H/^{15}N TROSY spectra of the ^{15}N,^{13}C-ErbB4tm/ErbB4tm "isotopic-heterodimer" embedded in the DMPC/DHPC lipid bicelles at L/P≈50, pH 5.0, 306 K (at *left*) and 323 K (at *right*). The ^{1}H–^{15}N side chain and backbone resonance assignments are shown (the water-exposed residues have an additional minor cross-peak due to the slow *cis-trans* transitions of the L^{644}–P^{645} peptide bond in the flexible N-terminal portion). At high temperature, the monomeric and dimeric sets of the ErbB4tm amide peaks merge to average peak positions because the monomer–dimer exchange process becomes fast on the NMR timescale. (B) Set of glycine regions of the ^{1}H/^{15}N TROSY spectra (dashed line in panel A) of ErbB4tm at L/P≈120, 60 and 40 (from *left* to *right*) acquired at 306 K, demonstrating the L/P-dependence of the equilibrium populations of the ErbB4tm monomeric and dimeric states. (**C**) G^{659} cross-peaks in the ^{1}H/^{15}N TROSY spectra of ErbB4tm (L/P≈50) acquired at temperatures between 288 and 323 K and their one-dimensional ^{1}H projections demonstrate the temperature dependence of the ErbB4tm monomer–dimer exchange process. The monomeric (*M*), dimeric (*D*) and higher oligomeric (presumably tetrameric, *T*) states are indicated.

exhibits the required distance between the C-termini of the TM helices (Fig. 2A). Notably, the polar amino acid substitution I658E, which results in a constitutively active receptor that induces the death of breast tumor cells *via* the enhancement of proapoptotic activity [20], is adjacent to the observed ErbB4 TM helix-packing interface (Fig. 2). Upon the dimerization of the I658E mutant ErbB4 form, the glutamate side chains likely participate in additional hydrogen bonding interactions with proximate polar groups of the opposite dimer subunit [46], thus enhancing helix–helix association and supporting uncontrolled receptor activity, although this has not been confirmed experimentally. In the observed dimer conformation, the side chain of V^{673}, the mutation of which completely abolishes the proapoptotic activity of ErbB4 [19], is exposed to the lipid environment, thus permitting proteolytic processing of the ErbB4 TM domain by the presenilin-dependent γ-secretase.

3.3. Interactions across the helix–helix interface induce a small bending of the ErbB4 transmembrane domain

The NOE cross-peak patterns for the monomeric and dimeric states of ErbB4tm are almost identical (excluding inter-monomeric NOEs), indicating that dimerization does not cause significant perturbations in the ErbB4tm structure. However, the chemical shifts of several amide

Table 1
Structural statistics for the ensemble of 20 best NMR structures of the ErbB4tm dimer in the DMPC/DHPC bicelles at 313 K and pH 5.0.

NMR distance and dihedral restraints	
Total unambiguous NOE restraints	522
Intra-residue	196
Inter-residue	310
Sequential ($\|i-j\|=1$)	142
Medium-range ($1<\|i-j\|\leq 4$)	152
Long-range ($\|i-j\|>4$)	0
Inter-monomeric	16
Hydrogen bond restraints (upper/lower)	136/136
Total torsion angle restraints	206
Backbone φ	84
Backbone ψ	84
Side chain χ^1	30
Side chain χ^2	8
Structure calculation statistics	
CYANA target function (Å^2)	0.9 ± 0.4
Restraint violations	
Distance (>0.2 Å)	2
Distance (>0.3 Å)	0
Dihedral (>5°)	0
Average pairwise r.m.s.d. (Å)	
α-helical region $(651–678)_2$	
Backbone atoms	0.22 ± 0.12
All heavy atoms	0.83 ± 0.17
Ramachandran analysis [a]	
% Residues in most favored regions	80.0
% Residues in additional allowed regions	17.7
% Residues in generously allowed regions	2.1 [b]
% Residues in disallowed regions	0.2 [b]
Helix–helix packing	
Contact surface area per monomer (Å^2)	360 ± 30
Angle θ between the helix axes (°)	-40 ± 2
Distance d between the helix axes (Å)	7.2 ± 0.3

[a] Ramachandran statistics was determined using CYANA program [30].
[b] Residues from unfolded and flexible regions.

protons change upon dimerization. The $^1H^N$ chemical shifts alter periodically in opposite directions along the protein sequence with a step of 3–4 residues (Figs. 2C and A.1), indicating changes in helical hydrogen bond lengths upon dimerization. Downfield $^1H^N$ chemical shifts (positive Δδ values) indicate shortened hydrogen bonds, while upfield shifts (negative Δδ values) indicate the formation of elongated hydrogen bonds upon helix dimerization. The observed $\delta(^1H^N)$ changes are rather small and do not exceed 0.1 ppm, corresponding to a maximum variation in the length of hydrogen bonds of 0.05 Å [52], which cannot be detected from the NOE data. Intriguingly, the perturbations of $\delta(^1H^N)$ are more pronounced in the vicinity of the dimerization interface and can be interpreted as local bending of the ErbB4tm helix upon dimer formation. The interfacial residues $A^{655}GxxGG^{660}$ form a polar cavity on the helix surface (Fig. 2B), which is unfavorably exposed to the hydrophobic lipid environment in the ErbB4tm monomer. Taking

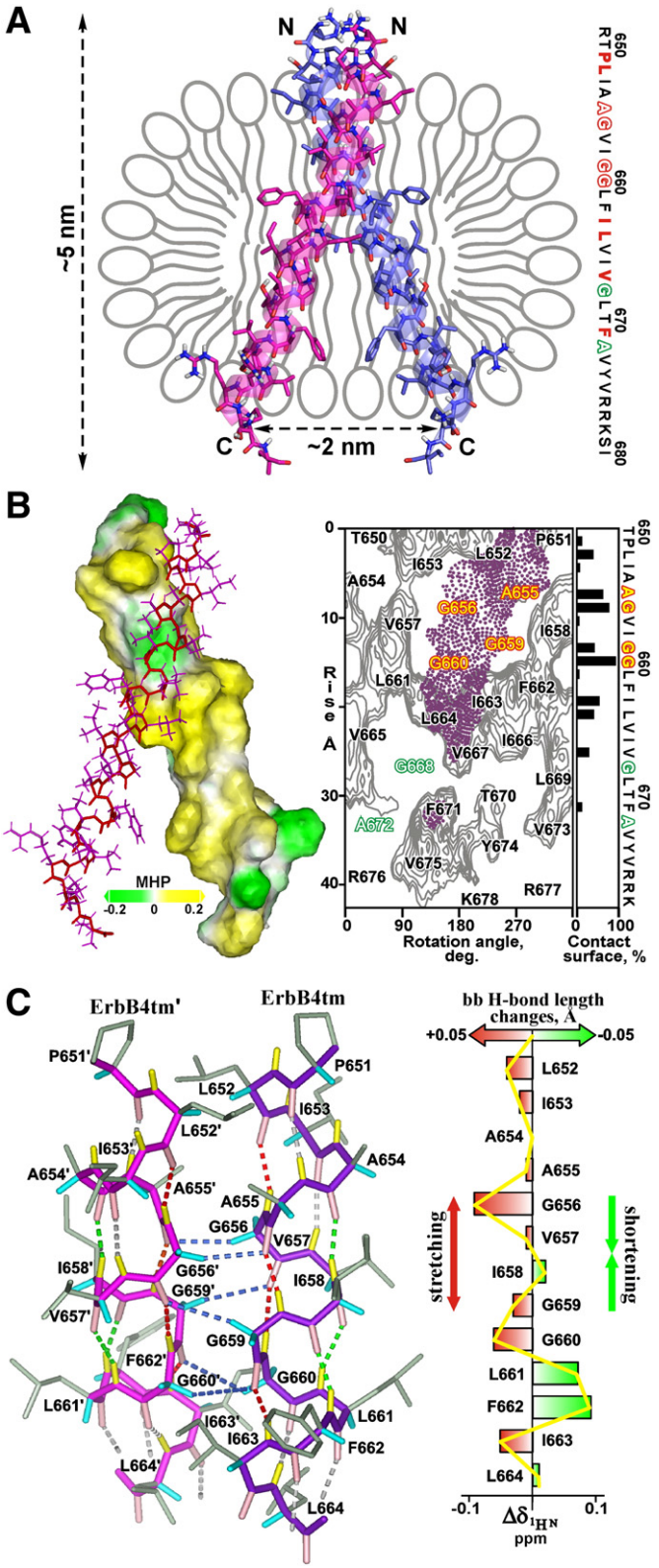

Fig. 2. NMR structure of the ErbB4tm dimer in the DMPC/DHPC bicellar environment. (A) Schematic representation of the supramolecular system of the ErbB4tm homodimer embedded in the bicelle. At *right*, the residues participating in the ErbB4tm association are highlighted by *red*. The N- and C-terminal characteristic GG4-like motifs $A^{655}GxxGG^{660}$ and $G^{668}xxxA^{672}$ are shown with *hollow* letters. (B) At *left*, hydrophobic and hydrophilic (polar) surfaces of the ErbB4tm dimer subunit are colored in *yellow* and *green*, respectively, according to molecular hydrophobicity potential (MHP) [33]. At *right* is the hydrophobicity map of the molecular surface of the ErbB4tm helix with contour isolines encircling hydrophobic regions with high values of MHP (see Section A.2). The map is presented in cylindrical coordinates associated with the TM helix. The ErbB4tm helix-packing interface is indicated by points. Residues composing N- and C-terminal dimerization GG4-like motifs $A^{655}GxxGG^{660}$ (employed) and $G^{668}xxxA^{672}$ (unemployed) are highlighted in *red-yellow* and *green*, respectively. Inter-monomeric contact surfaces of ErbB4tm residues are shown on the periphery (as a percentage of the total solvent-accessible area). (C) At *left*, the detailed structure of the ErbB4tm helix-packing interface. The formation of the network of inter-monomeric polar Cα—H···O contacts of the hydrogen-bond type (*blue* dotted lines) across the ErbB4tm dimer interface is accompanied by a structural "adjustment" (local bending) of the dimer subunits with periodical stretching (*red* dotted lines) and shortening (*green* dotted lines) of backbone hydrogen bonds of the TM helices. At *right*, the $^1H^N$ chemical shift differences between the dimer and monomer amide cross-peaks in the $^1H/^{15}N$ TROSY spectrum acquired for the ^{15}N-labeled ErbB4tm sample (at L/P≈50, 306 K and pH 5.0) indicate stretching and shortening of the helical hydrogen bonds upon dimerization.

into account the observed periodicity of the variation in hydrogen bond length, it can be assumed that the ErbB4tm span is bending slightly (likely straightening) when the polar surfaces of two TM helices associate tightly, forming a dimer interface that is shielded from the lipid tails.

The observed bending may represent an adjustment of the helical structure to optimize pairwise interactions across the dimerization interface. The adjustment is the result of contributions from polar contacts and van der Waals interactions and contributions from changes in the local helical structure of the individual helices to the free energy of the helix–helix interaction and may be inherent to the TM helix association employing the GG4-like motifs. This observation suggests that the helix–helix interaction in the membrane is determined not by simply matching the hydrophobic and hydrophilic properties of the interacting surfaces along with the steric compatibility of their landscapes but by the specific adjustment of the complementarities of the TM helices at the atomic level to permit the formation of polar contacts and tight helix–helix packing.

3.4. Thermodynamics of the monomer–dimer equilibrium of the ErbB4 transmembrane domain

To investigate the thermodynamics of the dimerization process of ErbB4tm in lipid bicelles, the observed monomer–dimer equilibrium was analyzed quantitatively. When the bicellar system behaves as a true solvent (sometimes referred to as "ideal" [38]), the dependence of the monomer–dimer equilibrium on $[Lip]_B$ should follow Eqs. (1) and (2) (see "Material and methods": Section 2.3) with a measure of ideality $\gamma = 1$ [36,38], assuming that the standard protein–micelle complex model is applicable to a lipid bicelle. This permits the introduction of the concept of standard free energy (ΔG_0) of the membrane protein association [38], which is equal to the apparent free energy of the process (ΔG_{app}) at 1 M $[Lip]_B$. When $\gamma = 1$, ΔG_0 can be directly derived from the so-called reduced association constant $K_{AR} = K_{app}[Lip]_B$ (according to Eqs. (3) and (4)).

The reduced association constant was measured for ErbB4tm in the wide range of the L/P ratio and total lipid concentration at 306 K, when the exchange process is not too fast and monomer–dimer cross-peaks are well separated but the signal broadening due to the deceleration of Brownian tumbling of the supramolecular system is not yet pronounced. The plot of the reduced association constant against the L/P ratio demonstrates that K_{AR} strongly decreases and becomes almost constant when less than one ErbB4tm molecule resides, on average, in one bicelle (consisting of ~100 lipids [40]) (Fig. 3A). This indicates that when two proteins are co-located in the same bicelle (as in "saturated" bicelles), either γ is not equal to unity or the reaction rate constants change for some reason. Notably, the saturation of bicelles by the peptide is accompanied by line broadening of the signals from the methyl groups of DMPC, indicating that the mobility of lipids is somehow restricted by the TM helices (Fig. A.7). The data obtained at a different L/P ratio and at the same bicellar lipid concentration revealed that the increase in K_{AR} is caused by the decrease in the L/P ratio and not the decrease in lipid concentration (Fig. 3A, Table 2), confirming that total lipid concentration and, therefore, non-ideal γ are not responsible for the observed dimer stabilization. The induced proximity of the TM segments (two or more proteins in the same bicelle) can be assumed to increase the probability of dimerization. Thus, the dimer fraction increases gradually with the number of bicelles with two monomers, which emerge due to the low L/P ratio.

The analysis of the obtained data in the framework of the described formalism demonstrates that, when less than one ErbB4tm resides in one bicelle, γ is close to unity ($\gamma = 1.0 \pm 0.1$ at L/P greater than 120), and ΔG_0 is equal to either -0.5 or -1.4 kcal mol^{-1}, depending on whether the concentration of protein in the lipid is calculated per long-chain lipids only or per total bicellar lipid, respectively. The long-chain lipids are believed to form a small bilayer in the bicelle [45]; however, the short-chain lipids forming the "rim" also likely play a role in

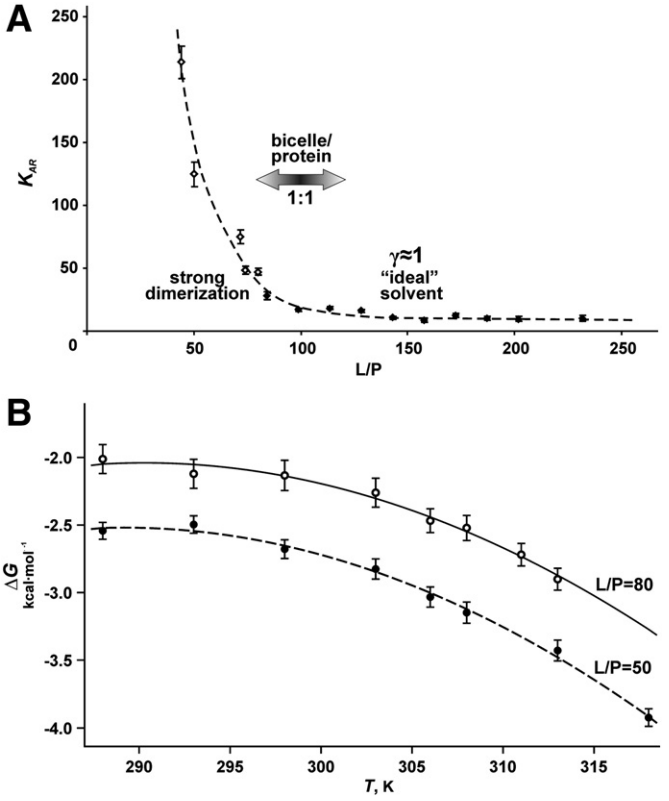

Fig. 3. Effects of the L/P ratio and temperature on the ErbB4tm monomer–dimer equilibrium. (A) The L/P-dependence of the reduced association constant, K_{AR}, monitored at 306 K demonstrates two characteristic regimes of the ErbB4tm dimerization process occur in the "saturated" and "unsaturated" bicelles at low and high L/P ratios, respectively. The K_{AR} values measured at constant bicellar lipid (93 mM) and protein (0.52 mM) concentrations are shown by *open* and *filled* boxes, respectively. The *dashed* line is the cubic spline fit of the data. (B) The temperature dependence of the free energy, Δ*G*, of the ErbB4tm dimerization at the L/P ratios of 50 (*dotted* line) and 80 (*solid* line) is fitted by Eq. (5).

accommodating the protein in the bicelle. These magnitudes can be compared to the dimerization free energies, which range from -2.4 to -3.7 kcal mol^{-1}, measured in different lipid bilayers for the TM domains of other RTK representatives: ErbB1, FGFR3 and EphA1 receptors [16,58–61]. The lower stability of the ErbB4tm dimer correlates well with the dimerization hierarchy of ErbB TM domains in LDAO micelles, in which the ErbB4tm homodimer is the least stable of all possible dimeric combinations within the family. The dimerization free energy of ErbB4tm is smaller than that of ErbB1tm by ~2 kcal mol^{-1} [11].

In addition to the dependence on L/P concentration, the temperature dependence (in the range of 288–323 K) of the reduced association constant (and, therefore, of the free energy of ErbB4tm dimerization) was investigated at two degrees of bicelle saturation with L/P of 50

Table 2
Thermodynamic parameters (at standard-state reference temperature T_0 of 298 K) of the monomer–dimer transition of ErbB4tm in the DMPC/DHPC environment at different degrees of the bicelle "saturation".

Parameter	Conditions 1	Conditions 2
Bicellar lipid concentration, mM	93 ± 5	93 ± 5
Protein concentration, mM	1.1 ± 0.1	1.9 ± 0.2
L/P ratio	80 ± 5	50 ± 3
K_{AR} (T_0)	47 ± 3	123 ± 8
ΔH_0, kcal mol^{-1}	5.4 ± 0.7	6.3 ± 0.7
ΔS_0, kcal mol^{-1} K^{-1}	0.025 ± 0.002	0.030 ± 0.002
$T_0\Delta S_0$, kcal mol^{-1}	7.5 ± 0.7	9.0 ± 0.6
ΔC_p, kcal mol^{-1} K^{-1}	0.96 ± 0.15	1.0 ± 0.1
ΔG, kcal mol^{-1}	−2.13 ± 0.15	−2.70 ± 0.1

and 80 at a total lipid bicellar concentration of 93 mM (Figs. 1C and 3B). Qualitatively, increasing temperatures favor dimerization, which is anticipated for an entropy-driven dimerization process. Moreover, beginning at 313 K, a higher oligomeric (presumably tetrameric) ErbB4tm complex becomes detectable as protein complex formation becomes progressively more energetically beneficial. Under both conditions, the curves describing the temperature dependence of the free energy of dimerization appeared to be strongly nonlinear, suggesting that the complex model should be employed for the data analysis. The diffusion measurements demonstrated that the bicelle hydrodynamic radius of ~2.5 nm remains unchanged in the temperature range of 288–323 K within the experimental uncertainty of 0.2 nm (Section A.4 and Fig. A.4), thus excluding the possibility that dimerization increases due to changes in the protein/bicelle ratio. A rather good fit of $\Delta G(T)$ was obtained with the relationship of Eq. (5), which assumes a temperature-dependent enthalpy $\Delta H(T)$ and entropy $\Delta S(T)$ of the process with constant heat capacity ΔC_p. The key thermodynamic parameters of the dimerization of ErbB4tm in a "saturated" bicellar environment at two L/P ratios and at a standard-state reference temperature T_0 of 298 K are summarized in Table 2. Clearly, in the "saturated" bicelles, the dimerization of ErbB4tm is endothermic and entropy-driven, with both entropy and enthalpy strongly dependent on the ambient temperature. Additionally, dimerization is enhanced by a decrease in the L/P ratio due to an increase in the favorable entropic contribution that exceeds the unfavorable enthalpy increase. This is the first detailed account of the thermodynamic parameters of TM helix dimerization in a "saturated" micelle/bicelle system, which are very distinct from the measurements conducted on the glycophorin A dimer in "unsaturated" micelles [37]. In some cases, the glycophorin A helix–helix interaction was accompanied by an increase in entropy, while an increase in enthalpy upon dimerization was not observed.

In conclusion, four main findings are reported in this section. First, the dimerization of the TM helices of ErbB4 in DMPC/DHPC bicelles obeys standard kinetics in dilute solutions and is enhanced when bicelles are saturated with peptide. Second, the dimerization process in "saturated" bicelles is endothermic. Third, the dimerization process in "saturated" bicelles is accompanied by increases in both entropy and heat capacity. And, fourth, the observed dimerization enhancement is due to an increase in the entropic contribution to the dimerization free energy. These findings are not obvious and require explanation. A possible interpretation of the obtained data is given in the following section.

3.5. Interpretation of the obtained thermodynamic parameters of ErbB4 transmembrane domain dimerization in a bicellar environment

3.5.1. Dimerization is accompanied by increases in both entropy and heat capacity

The observed increase in entropy may appear counterintuitive because it can be argued that protein oligomers are more ordered and less mobile than the separate monomers. Therefore, lipids are the only possible source of positive entropy for the dimerization process. Indeed, every TM helix is surrounded by a "coat" of lipids that is more or less tightly associated with the helix [53,62,63]. After the TM helices interact, a fraction of these "frozen" or to some degree spatially constrained lipids becomes more mobile because the accessible surface of the dimer is smaller (on 2×360 Å^2) than that of the two monomers and less lipid molecules can be attached to the surface. Thus, the TM helix association reduces the area of the protein–lipid interface and thereby increases the overall entropy of the system. The suggested hypothesis is supported by the considerable increase (≈1 kcal mol^{-1}K^{-1}) in the heat capacity upon dimerization. C_p is directly related to the number of degrees of freedom of a system. Dimerization itself would decrease the number of degrees of freedom of the protein, and the resulting increase in heat capacity may be the consequence of lipid release from the protein surface only. In a sense, the observed temperature curve is similar to the curves observed for the melting of globular proteins [41,64]. The described process may be represented as a partial melting of the protein–lipid complex that occurs upon TM helix dimerization. The presence of "frozen" lipids in our system is also supported by the lipid–protein NOE contacts observed for ErbB4tm in bicelles (Figs. A.1 and A.2). Indeed, the NOE is proportional to the rotational correlation time of the cross-relaxing nuclei, and the lipid–protein NOE cross-peak intensities, which are comparable to the inter-molecular protein–protein NOE cross-peak intensities in the dimer, imply that the protein–lipid interactions may have a lifetime similar to that of the protein–protein interactions. Therefore, we can conclude that the observed increase in entropy and heat capacity upon the dimerization of ErbB4tm is due to the change in the mobility of lipid molecules that are somehow associated with the protein surface.

3.5.2. The dimerization of ErbB4tm in saturated bicelles is endothermic

Computational studies and existing data on the energy of polar and van der Waals interactions demonstrate that protein–protein contacts should be favorable from the viewpoint of internal energy and decrease the system enthalpy [65–67]. In theory, some unfavorable interactions may occur at the helix–helix interface (i.e., coulombic repulsion between charged side chains [48,68] and interactions between helical dipoles). Nonetheless, the total enthalpic contribution to the TM helix–helix interaction is mostly dimer-supporting [14,37,69], and no adverse contacts could be observed in the spatial structure of the ErbB4tm dimer. Thus, in our system, the positive ΔH_0 may originate from either protein–lipid or lipid–lipid interactions. Protein–lipid contacts should be favorable, and the release of lipids from the protein surface upon dimerization will lead to an increase in enthalpy. Moreover, the lipid–lipid interactions in the ordered "coat" around the TM helices are also favorable from an internal energy perspective, and these interactions are destroyed to some extent upon helix association. In other words, we propose that the enthalpy of the lipid–protein–water system is increased upon dimerization due to the removal of lipid molecules from the protein surface and to the partial disruption of lipid–lipid interactions in the "coat" surrounding each TM helix.

3.5.3. The dimerization of ErbB4tm in saturated bicelles is enhanced due to an increase in dimerization entropy

The third finding that needs to be explained is the enhancement of the dimerization and increase in the dimerization entropy upon bicelle saturation. Here, we suggest two hypotheses. The first hypothesis states that dimerization enhances the degree of lipid ordering in the system, thus increasing the dimerization entropy. This suggestion is confirmed by literature data. An abrupt enhancement of TM helix dimerization was observed upon the transition from the liquid-crystal to the gel phase in DMPC bilayers [70]. Furthermore, the addition of cholesterol, which increases the ordering of lipid tails, to the lipid membranes favored dimerization [70–72]. The following mechanism may be responsible for this enhancement: when lipids are in the gel phase, the detachment of one lipid molecule from the surface of the TM helix will increase the mobility of other lipids because their movements in the gel phase are highly correlated and lipid–lipid interactions are strong. For TM helix–helix associations, this will result in greater dimerization entropy in comparison to dimerization in liquid crystalline lipids because more lipid molecules will become relatively mobile after the helix–helix interaction event.

The second hypothesis states that more ordered lipid molecules per protein are present in "saturated" bicelles than in "unsaturated" bicelles. Indeed, the increase in lipid ordering with bicelle saturation can be observed experimentally from the resonance broadening of the lipid tail groups at low L/P values (Fig. A7), which indicates decreasing mobility of the lipid tails. Additionally, according to molecular modeling data [73], the TM helix restricts the lipid mobility in a distance of ~2 nm, indicating that two monomers would essentially

affect every lipid in the ~5 nm bicelle (Fig. 5A, B). In a sense, such long-range ordering is similar to the behavior of lipids in the gel phase [63]. There may be several explanations for why two helices in one bicelle "freeze" more lipid molecules than two helices in separate bicelles, and the exact mechanism is outside the scope of the present work.

In summary, lipids are presumably more ordered in "saturated" bicelles, resulting in elevated dimerization entropy and enhanced dimerization in comparison to the "diluted" case. Similarly, the dimerization of ErbB4tm is enhanced dramatically when the L/P ratio decreases to the point of the statistically meaningful appearance of bicelles containing two proteins (approximately 100:1). Thus, low L/P ratios correspond to situations without a significant presence of a disordered lipid phase in the system, which causes a drastic enhancement of entropy-driven protein dimerization.

3.6. Steady-state kinetics of the monomer–dimer transition of the ErbB4 transmembrane domain

The relatively large difference in the chemical shifts of amide protons (≈0.11 ppm for G^{656}) in the dimeric and monomeric states permitted the measurement of the kinetic parameters of the dimerization. The exchange rate $k_{ex} = k_{diss} + k_{dim}M/[Lip]_B$, where k_{diss} and k_{dim} are rate constants of dissociation and dimerization, respectively, was measured from the intensities of the exchange cross-peaks in the ^{15}N-edited NOESY spectra (Fig. A.5) [27,42]. The reaction appeared to be rather slow ($k_{ex} \approx 30–40\ s^{-1}$), and the TM helix–helix association does occur that slowly under more native conditions, even on the timescale of seconds, as measured by fluorescence spectroscopy in phospholipid bilayers [74]. Rate constants were obtained at different protein and lipid concentrations at an optimal temperature of 306 K, when the accuracy was maximal (see Table 3). Because the measurements were made in "saturated" bicelles, the dimerization rate should increase with the degree of saturation, while the dissociation rate should remain unchanged, which is within the experimental error in agreement with the acquired data (see note in Table 3). Moreover, at low L/P values, neither dissociation nor dimerization depends on the frequency (~$10^5\ s^{-1}$ as estimated from the Stokes–Einstein equation) of collisions between bicelles. Indeed, while the bicelle concentration and, therefore, the collision frequency decreased two-fold, the dissociation rate remained almost unchanged, as did the dimerization rate constant (Table 3).

The temperature dependence of the dimerization rate constant k_{dim} in the "saturated" state (at L/P of 50) was monitored at 298–313 K by line shape analysis (Fig. A.6). The dependence appeared to follow the Arrhenius equation with an activation energy $E_a \approx 28$ kcal mol^{-1} (Fig. 4A). Treatment of the obtained data from the perspective of transition state theory according to the Eyring equation, Eq. (8) (with the transmission coefficient $\kappa = 1$), yielded the free energy barrier accompanying the ErbB4tm association, $\Delta G_A^{\ddagger} \approx 13$ kcal mol^{-1}, which gradually decreases as the temperature increases (Fig. 4B). The barrier appeared to be extremely high in comparison with theoretical estimates from molecular modeling (up to ~2 kcal mol^{-1} [75]). However, the dimerization itself requires partial desolvation of the interacting

Table 3
Steady-state kinetics of the monomer–dimer transition of ErbB4tm in the "saturated" DMPC/DHPC bicelles measured based on the exchange cross-peaks in the ^{15}N-edited NOESY spectra acquired at 306 K.

Parameter	Conditions 1	Conditions 2[a]	Conditions 3[b]
Bicellar lipid concentration, mM	93 ± 5	93 ± 5	47 ± 5
Protein concentration, mM	1.3 ± 0.1	2.1 ± 0.2	0.7 ± 0.1
L/P ratio[c]	71 ± 5	44 ± 5	71 ± 5
K_{AR}	39 ± 6	100 ± 20	35 ± 8
k_{diss}, s^{-1}	23 ± 3	22 ± 3	27 ± 6
k_{dim}, s^{-1}	900 ± 150	2200 ± 300	950 ± 200
k_{ex}, s^{-1}	30 ± 4	37 ± 5	40 ± 8

[a] Transition from condition nos. 1 to 2. At fixed bicellar lipid concentration the $k_{diss} \approx 23\ s^{-1}$ is practically insensitive to the reduction of the L/P ratio in 1.6 times whereas k_{dim} has grown twice.

[b] Transition from condition nos. 1 to 3. The two-fold dilution of the ErbB4tm sample reveals similar dimerization parameters, since the L/P ratio and hence the fraction of bicelles with two proteins remained unchanged.

[c] When the bicelles behave as an "ideal" solvent (at L/P > 120), the kinetic parameters are out of accurate measurement due to low fraction of the dimer observed at these conditions.

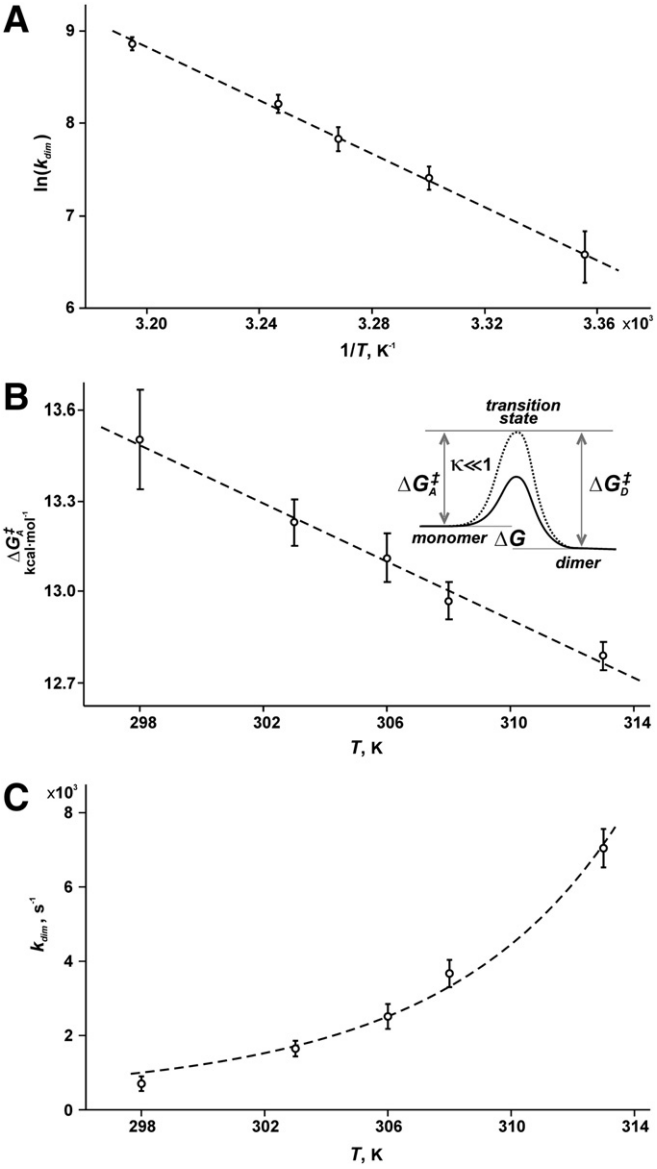

Fig. 4. Equilibrium kinetics of the monomer–dimer transition of ErbB4tm in the DMPC/DHPC bicellar environment. (A) The temperature dependence of the dimerization rate constant k_{dim} obtained in the "saturated" case (L/P ≈ 50) from the line shape analysis of the G^{656} cross-peaks in the ^{1}H/^{15}N TROSY spectra is fitted by the Arrhenius equation with an activation energy E_a equal to 28 ± 2 kcal mol^{-1}. (B) Temperature dependence of the free energy $\Delta G_A^{\ddagger}$ of the transition state accompanying the ErbB4tm association. The $\Delta G_A^{\ddagger}$ values were estimated from the dimerization rate constant k_{dim} according to the Eyring equation (Eq. (8)), with the transmission coefficient κ equal to 1. Protein folding or helix–helix dimerization may be characterized by κ values much smaller than unity, which greatly increases the apparent value of the free energy barrier of the processes, as represented by the contrast between the *solid* (physical barrier) and *dotted* (apparent barrier) lines in the right top corner scheme. (C) The temperature dependence of the dimerization rate constant k_{dim} is fitted simultaneously by Eqs. (5) and (8), assuming that $\Delta S_A^{\ddagger}$ and $\Delta C_p^{\ddagger}$ for the transition state are not higher than $\Delta S_0 \approx 0.03$ kcal·mol^{-1}K^{-1} and $\Delta C_p \approx 1$ kcal mol^{-1}K^{-1} (as estimated for the ErbB4tm dimerization).

TM helices from lipids and, as was shown above, is definitely associated with local changes in the monomer spatial structure, which both contribute to the activation barrier. Nevertheless, we suppose that the barrier obtained from the simplest approximation of activation is an overestimate in our case. In fact, complex reactions such as protein folding or helix–helix dimerization are characterized by κ values (probability of the reaction taking place once the system has reached the activated state) much smaller than unity. For example, for water-soluble helical bundles, a commonly accepted generic value is $\kappa \approx 1.6\times10^{-7}$ [44]. The use of this generic value of κ additively decreases the $\Delta G_A^{\ddagger}$ by approximately 9 kcal mol^{-1}. Taking into account the temperature dependence (Eq. (5)) of both the entropy and enthalpy of the transient state and reconciling the physical models of the excitation and dimerization processes permits an estimate of a lower limit of $\kappa \geq 3\times10^{-5}$ (Fig. 4C), which yields a minimal $\Delta G_A^{\ddagger} \approx 7$ kcal mol^{-1} with $\Delta H_A^{\ddagger} \approx 16$ kcal mol^{-1} and $T_0\Delta S_A^{\ddagger} \approx 9$ kcal mol^{-1} (for details see Section A.5). The magnitude of κ appears to be the same for globular proteins or even one to two orders greater because the TM helices are already formed and inserted into the membrane prior to the dimerization process (according to the two-stage model of membrane protein folding [14]). Although more thorough kinetic measurements are desirable for an accurate description of the thermodynamics of a transition state during specific TM helix recognition and to determine a more precise value of κ, the present study is the first to obtain the kinetic and thermodynamic parameters of the interaction between TM helices. The self-consistency of the acquired data derived by different experimental approaches is confirmed by the fact that applying an Eyring formalism to the reverse process and using the value of the dissociation constant derived from exchange NMR spectroscopy data, approximately 23 s^{-1} (Table 3), we obtain the free energy barrier to dissociation, $\Delta G_D^{\ddagger}$, which is equal to 9.6 kcal mol^{-1} at 298 K (assuming $\kappa = 3\times10^{-5}$). When this value is subtracted from the association free energy barrier $\Delta G_A^{\ddagger}$ estimated above, the dimerization free energy $\Delta G \approx -2.6$ kcal mol^{-1} is obtained, which is in very good agreement with the state population-based equilibrium constants at L/P $\approx$ 50.

This large difference between $\Delta H_A^{\ddagger}$ and ΔH_0 (at least 10 kcal mol^{-1}) suggests that the favorable specific pairwise interactions (e.g., van der Waals and polar interactions) at the dimerization interface of ErbB4tm contribute greatly to the thermodynamics of dimerization. After the barrier is passed, favorable and "specific" protein–protein interactions enter the process and lower the enthalpy of the system to the final value of the enthalpy of dimerization. Therefore, the difference between the enthalpy of the transition state and the enthalpy of dimerization is a lower estimate of the enthalpy of protein–protein interaction. Notably, the theoretical estimates obtained for the energy of TM helix–helix interaction range around the same value, approximately 10 kcal mol^{-1} [65,67]. Thus, the entropy-driven character of the observed dimerization process contradicts neither the specific character of dimerization nor the determinant role of enthalpic contribution in the TM helix–helix association in a "saturated" bicellar environment (for details see Section A.5).

3.7. Microcompartmentalization can affect "weak" dimerization of protein transmembrane domains

To summarize, the dependence of the dimerization propensity on the concentration of ErbB4tm in the lipid has two distinct modes. In "unsaturated" bicelles, the reduced association constant K_{AR} remains invariable but begins to increase once significant numbers of bicelles containing more than one ErbB4tm molecule appear and lipids become less mobile (Fig. 3A). The relatively slow process of TM helix dimerization (associated with a high apparent activation barrier) in the bicellar environment can explain the substantial difference in the association constants observed in the "diluted" and "saturated" cases. For the dimerization process to occur, two monomers need to spend, on average, tens of milliseconds in the same bicelle in the form of a certain precomplex surrounded by "frozen" lipids. Over this period of time, the bicelle would experience thousands of collisions with other bicelles, and at least some of these collisions would presumably be accompanied by partial fusion and the exchange of substance between bicelles. In the "diluted" case, the bicelles would behave as a liquid crystalline lipid bilayer with an "ideal" solvent property, whereas in the "saturated" case, the dimerization would always be enhanced due to some degree of ordering of all lipids in the bicelles (Fig. 5A, B).

The increase in the association constant with the protein saturation of the membrane-mimicking environment was also observed for the left-handed dimer of ErbB3tm in DPC micelles [15]; the only difference was that, in case of the right-handed ErbB4tm dimer, the value of γ is close to unity, implying that the bicelles in this case behave as an "ideal" solvent. Therefore, in the "unsaturated" range of concentrations, the lipid bicelles can be used to measure the kinetics and thermodynamics of weakly interacting TM proteins by NMR; these parameters may be compared to the thermodynamic parameters of various TM helix interactions measured by other techniques.

In addition, the results obtained for bicelles at "saturated" concentrations of ErbB4tm may be of even greater biological relevance compared to seemingly ideal model systems such as liposomes or "unsaturated" bicelles. The substantial increase in the dimerization rate constant in bicelles with more than one protein molecule is caused mostly by the beneficial entropic contribution in the presumably more ordered lipid environment. Lipid ordering in biological membranes varies greatly depending on the temperature, local lipid composition and presence of membrane proteins. In cellular membranes, proteins do not freely diffuse but rather cluster together in membrane microdomains such as rafts, caveolae or signaling platforms based on their function or physical properties (e.g., the localization of ErbB4 and associated signaling molecules in the lipid rafts [18]). Accordingly, the degree of ordering of lipids in such microdomains will substantially affect TM helix–helix interactions, especially for single-span membrane proteins. Therefore, partitioning of the protein into one of these domains can serve as a trigger for the protein dimerization underlying its biological function.

Substantial enhancement of dimerization in the ordered lipid environment suggests that, if the TM protein preferentially partitions into the more ordered microdomain, it would greatly amplify the effect of the weak TM helix–helix interactions by simultaneously increasing the entropic contribution to the free energy of the TM helix–helix association and restricting the protein localization to a small fraction of the overall membrane surface (a certain "depletion effect" [76]). The situation with "saturated" bicelles (micelles) essentially mimics the behavior of the protein in these membrane microdomains from both perspectives (Fig. 5C). Such mechanisms can explain how seemingly weak TM helix–helix interactions may play an important role in overall protein function or, alternatively, in the inhibition of the protein's biological activity, which can have practical implications [2,77].

The dimerization process is fairly slow, as observed both in bicelles and liposomes [74], and the corresponding apparent (kinetically derived) energy barrier is accordingly high. This would slow down ligand-induced dimerization and may explain the existence of some of the interacting membrane proteins in the form of pre-complexes that are ready for immediate activation (e.g., preformed but inactive homo- and heterodimers of the ErbB receptor tyrosine kinases detected in living cells [8]).

4. Conclusions

The obtained structural, kinetic and thermodynamic data concerning the dimerization of ErbB4tm in small lipid bicelles provide insights into the folding processes of a single-span helical TM domain in a model environment and, perhaps, in cellular membranes. The phospholipid bicelles occupied by less than one protein proved to behave as an "ideal" solvent for the association of the ErbB4tm helices, while

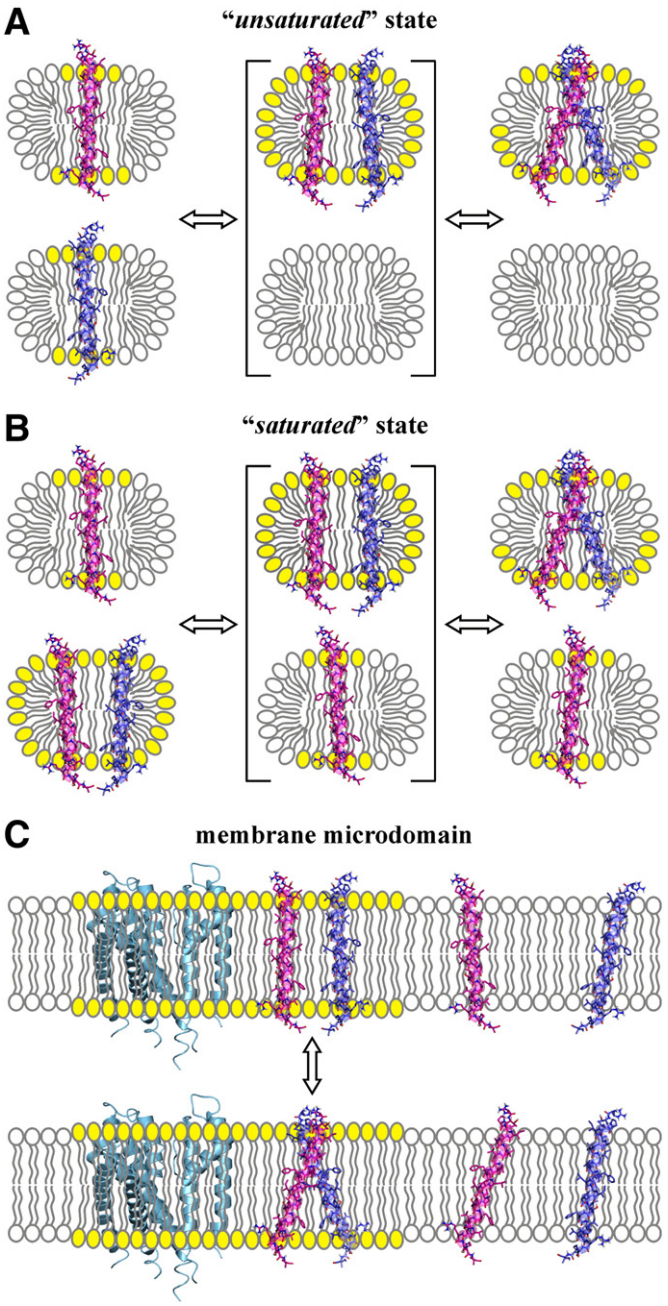

Fig. 5. Schematic representation of the association process of the TM single-span protein in "unsaturated" (A) and "saturated" (B) states of the bicellar environment as well as in the membrane microdomains (C). Lipids in the ordered phase are highlighted in *yellow*. When the L/P ratio is high (A), many "empty" bicelles come into contact with bicelles containing a pair of monomers, and frequent bicellar collisions are much more likely to disturb or destroy a helix–helix precomplex surrounded by "frozen" lipids, dissolving it in a generally less ordered lipid environment, and the entropy of the monomeric state is increased due to the reduction in lipid ordering. In other words, in the "diluted" case, the fraction of "successful attempts" to dimerize is efficiently reduced by premature dissolution of some of the interacting pairs before the reaction can occur. In the "saturated" case (B), by contrast, bicelles with interacting monomers collide primarily with bicelles that also contain one or more protein molecules. The lipids in these bicelles are also ordered by the interaction with the protein and therefore have a much smaller propensity to destroy the ordered phase in another bicelle; thus, when bicelles collide, the ordering of the lipid fraction remains unchanged. Thus, the slow character of the TM helix–helix interaction permits the observed concentration-dependent entropic enhancement of the TM dimerization. The protein dimerization in the "saturated" membrane-mimicking environment presumably resembles the behavior of the protein in membrane microdomains, which are characterized by more ordered lipids and the presence of other membrane proteins (C).

multiply occupied bicelles (the "saturated" case at low L/P ratio) are more similar to the microdomains of the ordered lipid phase in cellular membranes, providing substantial entropy-driven enhancement of the weak helix–helix interactions. The equilibrium kinetics of the monomer–dimer transition of ErbB4tm also reveal that, despite the rather low value of the dimerization free energy, there is a high apparent activation barrier for the dimerization and dissociation of TM helices. The temperature dependence of the dimerization in "saturated" bicelles revealed that the process is entropy-driven and is accompanied by an increase in the protein–lipid system heat capacity. In bicelles, the ErbB4 TM domain self-associates *via* the N-terminal double GG4-like motif in a fashion similar to the homo- and heterodimerization of the ErbB2 and ErbB1/ErbB2 TM domains, with the helix–helix arrangement presumably corresponding to the receptor active state. The dimerization proceeds through the structural "adjustment" of the dimer subunits, resulting in the local bending of the ErbB4 TM span and tight helix–helix association with the formation of a network of inter-monomeric polar and van der Waals contacts, which may be inherent for TM domains interacting via GG4-like motifs. The example of ErbB4tm demonstrates clearly that lipid-related effects cannot be ignored when free energy is estimated for TM helix–helix interactions in integral membrane proteins.

5. Accession numbers

The chemical shift assignments, NMR-derived constraints and atomic coordinates of the ErbB4tm homodimer have been deposited in the Biological Magnetic Resonance Data Bank (BMRB ID: 7205) and the Protein Data Bank (PDB ID: 2LCX).

Acknowledgements

The authors are grateful to Schulga A.A., Ermolyuk Ya.S. and Tkach E.N. for providing the technique for the expression and purification of the bitopic protein TM fragments; Chupin V.V. for the synthesis of the deuterium-labeled lipids; and Volynsky P.E., Lesovoy D.M., and Pavlov K.V. for assistance with the preparation of the manuscript.

Funding Sources: This work was supported by the Russian Foundation for Basic Research (12-04-01816), the Program of the Russian Academy of Science "Molecular and Cellular Biology", the Russian Funds Investment Group, the Federal Target Programs "Scientific and Pedagogical Specialists of Innovation Russia (2009–2013)" (P1276 and 16.740.11.0195) and the "Research and development in priority fields of Russian scientific and technological complex in 2007–2013" (16.512.11.2172). Bocharov E.V. personally thanks Beirit K.A. for financial support.

Appendix A. Supplementary data

Description of some details of methods used and results obtained for ErbB4tm embedded into the bicelles is presented in Sections A.1–A.5, Table A.1, and Figs. A.1–A.6. Supplementary data to this article can be found online at http://dx.doi.org/10.1016/j.bbamem.2012.05.001.

References

[1] A. Rath, R.M. Johnson, C.M. Deber, Peptides as transmembrane segments: decrypting the determinants for helix–helix interactions in membrane proteins, Biopolymers 88 (2007) 217–232.
[2] A. Bennasroune, M. Fickova, A. Gardin, S. Dirrig-Grosch, D. Aunis, G. Cremel, P. Hubert, Transmembrane peptides as inhibitors of ErbB receptor signaling, Mol. Biol. Cell 15 (2004) 3464–3474.
[3] E. Li, K. Hristova, Role of receptor tyrosine kinase transmembrane domains in cell signaling and human pathologies, Biochemistry 45 (2006) 6241–6251.
[4] J. Schlessinger, Cell signaling by receptor tyrosine kinases, Cell 281 (2000) 211–225.
[5] J.M. Mendrola, M.B. Berger, M.C. King, M.A. Lemmon, The single transmembrane domains of ErbB receptors self-associate in cell membranes, J. Biol. Chem. 277 (2002) 4704–4712.

[6] T. Moriki, H. Maruyama, I.N. Maruyama, Activation of preformed EGF receptor dimers by ligand-induced rotation of the transmembrane domain, J. Mol. Biol. 311 (2001) 1011–1026.
[7] S.J. Fleishman, J. Schlessinger, N. Ben-Tal, A putative molecular-activation switch in the transmembrane domain of ErbB2, Proc. Natl. Acad. Sci. U. S. A. 99 (2002) 15937–15940.
[8] R.H. Tao, I.N. Maruyama, All EGF (ErbB) receptors have preformed homo- and heterodimeric structures in living cells, J. Cell Sci. 121 (2008) 3207–3217.
[9] M.A. Olayioye, R.M. Neve, H.A. Lane, N.E. Hynes, The ErbB signaling network: receptor heterodimerization in development and cancer, EMBO J. 19 (2000) 3159–3167.
[10] C.M. Warren, R. Landgraf, Signaling through ERBB receptors: multiple layers of diversity and control, Cell. Signal. 18 (2006) 923–933.
[11] J.P. Duneau, A.P. Vegh, J.N. Sturgis, A dimerization hierarchy in the transmembrane domains of the HER receptor family, Biochemistry 46 (2007) 2010–2019.
[12] D. Gerber, N. Sal-Man, Y. Shai, Two motifs within a transmembrane domain, one for homodimerization and the other for heterodimerization, J. Biol. Chem. 279 (2004) 21177–21182.
[13] C. Escher, F. Cymer, D. Schneider, Two GxxxG-like motifs facilitate promiscuous interactions of the human ErbB transmembrane domains, J. Mol. Biol. 389 (2009) 10–16.
[14] K.R. MacKenzie, Folding and stability of alpha-helical integral membrane proteins, Chem. Rev. 106 (2006) 1931–1977.
[15] K.S. Mineev, N.F. Khabibullina, E.N. Lyukmanova, D.A. Dolgikh, M.P. Kirpichnikov, A.S. Arseniev, Spatial structure and dimer–monomer equilibrium of the ErbB3 transmembrane domain in DPC micelles, Biochim. Biophys. Acta 1808 (2011) 2081–2088.
[16] L. Chen, M. Merzlyakov, T. Cohen, Y. Shai, K. Hristova, Energetics of ErbB1 transmembrane domain dimerization in lipid bilayers, Biophys. J. 96 (2009) 4622–4630.
[17] G. Carpenter, ErbB-4: mechanism of action and biology, Exp. Cell Res. 284 (2003) 66–77.
[18] L. Ma, Y.Z. Huang, G.M. Pitcher, J.G. Valtschanoff, Y.H. Ma, L.Y. Feng, B. Lu, W.C. Xiong, M.W. Salter, R.J. Weinberg, L. Mei, R.J. Weinberg, L. Mei, Ligand-dependent recruitment of the ErbB4 signaling complex into neuronal lipid rafts, J. Neurosci. 23 (2003) 3164–3175.
[19] G.A. Vidal, D.E. Clark, L. Marrero, F.E. Jones, Presenilin-dependent gamma-secretase processing regulates multiple ERBB4/HER4 activities, J. Biol. Chem. 280 (2005) 19777–19783.
[20] G.A. Vidal, A. Naresh, L. Marrero, F.E. Jones, A constitutively active ERBB4/HER4 allele with enhanced transcriptional coactivation and cell-killing activities, Oncogene 26 (2007) 462–466.
[21] M. Sundvall, K. Iljin, S. Kilpinen, H. Sara, O.P. Kallioniemi, K.J. Elenius, Role of ErbB4 in breast cancer, J. Mammary Gland Biol. Neoplasia 13 (2008) 259–268.
[22] M.V. Goncharuk, A.A. Schulga, Ya.S. Ermolyuk, E.N. Tkach, Yu.E. Pustovalova, K.S. Mineev, E.V. Bocharov, I.V. Maslennikov, A.S. Arseniev, M.P. Kirpichnikov, Bacterial synthesis, purification and solubilization of transmembrane segments of ErbB family members, Mol. Biol. (rus) 45 (2011) 823–832.
[23] K.J. Glover, J.A. Whiles, G. Wu, N. Yu, R. Deems, J.O. Struppe, R.E. Stark, E.A. Komives, R.R. Vold, Structural evaluation of phospholipid bicelles for solution-state studies of membrane-associated biomolecules, Biophys. J. 81 (2001) 2163–2171.
[24] P. Chakrabarti, G. Khorana, A new approach to the study of phospholipid-protein interactions in biological membranes. Synthesis of fatty acids and phospholipids containing photosensitive groups, Biochemistry 14 (1975) 5021–5033.
[25] R.L.J. Keller, The Computer Aided Resonance Assignment Tutorial, CANTINA Verlag, Goldau, Switzerland, 2004.
[26] M. Sattler, J. Schleucher, C. Griesinger, Heteronuclear multidimensional NMR experiments for the structure determination of proteins in solution employing pulsed field gradients, Prog. Nucl. Magn. Reson. Spectrosc. 34 (1999) 93–158.
[27] J. Cavanagh, W.J. Fairbrother, A.G. Palmer, N.J. Skelton, Protein NMR Spectroscopy, Principles and Practice, second ed. Academic Press, San Diego, CA, U.S.A., 2006
[28] V.Y. Orekhov, D.E. Nolde, A.P. Golovanov, D.M. Korzhnev, A.S. Arseniev, Processing of heteronuclear NMR relaxation data with the new software DASHA, Appl. Magn. Reson. 9 (1995) 581–588.
[29] N.A. Farrow, R. Muhandiram, A.U. Singer, S.M. Pascal, C.M. Kay, G. Gish, S.E. Shoelson, T. Pawson, J.D. Forman-Kay, L.E. Kay, Backbone dynamics of a free and phosphopeptide-complexed Src homology 2 domain studied by 15N NMR relaxation, Biochemistry 33 (1994) 5984–6003.
[30] P. Güntert, Automated NMR protein structure calculation, Prog. Nucl. Magn. Reson. Spectrosc. 43 (2003) 105–125.
[31] C. Zwahlen, P. Legault, S.J.F. Vincent, J. Greenblatt, R. Konrat, L.E. Kay, Methods for measurement of inter-molecular NOEs by multinuclear NMR spectroscopy: application to a bacteriophage λ N-peptide/boxB RNA complex, J. Am. Chem. Soc. 119 (1997) 6711–6721.
[32] G. Cornilescu, F. Delaglio, A. Bax, Protein backbone angle restraints from searching a database for chemical shift and sequence homology, J. Biomol. NMR 13 (1999) 289–302.
[33] R.G. Efremov, G. Vergoten, Hydrophobic nature of membrane-spanning α-helical peptides as revealed by Monte Carlo simulations and molecular hydrophobicity potential analysis, J. Phys. Chem. 99 (1995) 10658–10666.
[34] W. Kabsch, C. Sander, Dictionary of protein secondary structure: pattern recognition of hydrogen-bonded and geometrical features, Biopolymers 22 (1983) 2577–2637.
[35] R. Koradi, M. Billeter, K. Wüthrich, A program for display and analysis of macromolecular structures, J. Mol. Graph. 14 (1996) 51–55.
[36] D. Josse, C. Ebel, D. Stroebel, A. Fontaine, F. Borges, A. Echalier, D. Baud, F. Renault, M. Le Maire, E. Chabrieres, P. Masson, Oligomeric states of the detergent-solubilized human serum paraoxonase (PON1), J. Biol. Chem. 277 (2002) 33386–33397.
[37] L.E. Fisher, D.M. Engelman, J.N. Sturgis, Effect of detergents on the association of the glycophorin a transmembrane helix, Biophys. J. 85 (2003) 3097–3105.
[38] K.G. Fleming, Standardizing the free energy change of transmembrane helix–helix interactions, J. Mol. Biol. 323 (2002) 563–571.
[39] A.M. Stanley, K.G. Fleming, The process of folding proteins into membranes: challenges and progress, Arch. Biochem. Biophys. 469 (2008) 46–66.
[40] E.V. Bocharov, Y.E. Pustovalova, K.V. Pavlov, P.E. Volynsky, M.V. Goncharuk, Y.S. Ermolyuk, D.V. Karpunin, A.A. Schulga, M.P. Kirpichnikov, R.G. Efremov, I.V. Maslennikov, A.S. Arseniev, Unique dimeric structure of BNip3 transmembrane domain suggests membrane permeabilization as a cell death trigger, J. Biol. Chem. 282 (2007) 16256–16266.
[41] W.J. Becktel, J.A. Schellman, Protein stability curves, Biopolymers 26 (1987) 1859–1877.
[42] G.S. Rule, T.K. Hitchens, Fundamentals of Protein NMR Spectroscopy (Focus on Structural Biology), Springer, Netherlands, 2006, pp. 411–414.
[43] H. Eyring, The activated complex and the absolute rate of chemical reactions, Chem. Rev. 17 (1935) 65–77.
[44] W.Y. Choy, Z. Zhou, Y. Bai, L.E. Kay, An 15N NMR spin relaxation dispersion study of the folding of a pair of engineered mutants of apocytochrome b562, J. Am. Chem. Soc. 127 (2005) 5066–5072.
[45] R.S. Prosser, F. Evanics, J.L. Kitevski, M.S. Al-Abdul-Wahid, Current applications of bicelles in NMR studies of membrane-associated amphiphiles and proteins, Biochemistry 45 (2006) 8453–8465.
[46] E.V. Bocharov, K.S. Mineev, P.E. Volynsky, Ya.S. Ermolyuk, E.N. Tkach, A.G. Sobol, V.V. Chupin, M.P. Kirpichnikov, R.G. Efremov, A.S. Arseniev, Spatial structure of the dimeric transmembrane domain of the growth factor receptor ErbB2 presumably corresponding to the receptor active state, J. Biol. Chem. 283 (2008) 6950–6956.
[47] K.S. Mineev, E.V. Bocharov, Y.E. Pustovalova, O.V. Bocharova, V.V. Chupin, A.S. Arseniev, Spatial structure of the transmembrane domain heterodimer of ErbB1 and ErbB2 receptor tyrosine kinases, J. Mol. Biol. 400 (2010) 231–243.
[48] E.V. Bocharov, M.L. Mayzel, P.E. Volynsky, M.V. Goncharuk, Y.S. Ermolyuk, A.A. Schulga, E.O. Artemenko, R.G. Efremov, A.S. Arseniev, Spatial structure and pH-dependent conformational diversity of dimeric transmembrane domain of the receptor tyrosine kinase EphA1, J. Biol. Chem. 283 (2008) 29385–29395.
[49] E.V. Bocharov, M.L. Mayzel, P.E. Volynsky, K.S. Mineev, E.N. Tkach, Y.S. Ermolyuk, A.A. Schulga, R.G. Efremov, A.S. Arseniev, Left-handed dimer of EphA2 transmembrane domain: helix packing diversity among receptor tyrosine kinases, Biophys. J. 98 (2010) 881–889.
[50] T. Zhuang, B.K. Jap, C.R. Sanders, Solution NMR approaches for establishing specificity of weak heterodimerization of membrane proteins, J. Am. Chem. Soc. 133 (2011) 20571–20580.
[51] N. Jura, N.F. Endres, K. Engel, S. Deindl, R. Das, M.H. Lamers, D.E. Wemmer, X. Zhang, J. Kuriyan, Mechanism for activation of the EGF receptor catalytic domain by the juxtamembrane segment, Cell 137 (2009) 1293–1307.
[52] D.S. Wishart, B.D. Sykes, F.M. Richards, Relationship between nuclear magnetic resonance chemical shift and protein secondary structure, J. Mol. Biol. 222 (1991) 311–333.
[53] S.H. White, W.C. Wimley, Membrane protein folding and stability: physical principles, Annu. Rev. Biophys. Biomol. Struct. 28 (1999) 319–365.
[54] A. Senes, I. Ubarretxena-Belandia, D.M. Engelman, The Cα–H···O hydrogen bond: a determinant of stability and specificity in transmembrane helix interactions, Proc. Natl. Acad. Sci. U. S. A. 98 (2001) 9056–9061.
[55] A. Senes, D.E. Engel, W.F. DeGrado, Folding of helical membrane proteins: the role of polar, GxxxG-like and proline motifs, Curr. Opin. Struct. Biol. 14 (2004) 465–479.
[56] K.R. MacKenzie, J.H. Prestegard, D.M. Engelman, A transmembrane helix dimer: structure and implications, Science 276 (1997) 131–133.
[57] A.M. Stanley, K.G. Fleming, The transmembrane domains of ErbB receptors do not dimerize strongly in micelles, J. Mol. Biol. 347 (2005) 759–772.
[58] R. Soong, M. Merzlyakov, K. Hristova, Hill coefficient analysis of transmembrane helix dimerization, J. Membr. Biol. 230 (2009) 49–55.
[59] E.O. Artemenko, N.S. Egorova, A.S. Arseniev, A.V. Feofanov, Transmembrane domain of EphA1 receptor forms dimers in membrane-like environment, Biochim. Biophys. Acta 1778 (2008) 2361–2367.
[60] E. Li, M. You, K. Hristova, SDS-PAGE and FRET suggest weak interactions between FGFR3 TM domains in the absence of extracellular domains and ligands, Biochemistry 44 (2005) 352–360.
[61] E. Li, K. Hristova, Receptor tyrosine kinase transmembrane domains: function, dimer structure and dimerization energetics, Cell Adh. Migr. 4 (2010) 249–254.
[62] M.R. Morrow, J.C. Huschilt, J.H. Davis, Simultaneous modeling of phase and calorimetric behavior in an amphiphilic peptide/phospholipid model membrane, Biochemistry 24 (1985) 5396–5406.
[63] S.A. Simon, T.J. McIntosh, Peptide–Lipid Interactions, Elsevier Science, San Diego, CA, U.S.A., 2002.
[64] A.R. Fersht, Structure and Mechanism in Protein Science, W.H. Freeman and Company, New York, U.S.A., 1999.
[65] A.L. Lomize, I.D. Pogozheva, H.I. Mosberg, Quantification of helix–helix binding affinities in micelles and lipid bilayers, Protein Sci. 13 (2004) 2600–2612.
[66] R.G. Efremov, Y.A. Vereshaga, P.E. Volynsky, D.E. Nolde, A.S. Arseniev, Association of transmembrane helices: what determines assembling of a dimer? J. Comput. Aided Mol. Des. 20 (2006) 27–45.
[67] J. Zhang, T. Lazaridis, Calculating the free energy of association of transmembrane helices, Biophys. J. 91 (2006) 1710–1723.
[68] W.C. Peng, X. Lin, J. Torres, The strong dimerization of the transmembrane domain of the fibroblast growth factor receptor (FGFR) is modulated by C-terminal juxtamembrane residues, Protein Sci. 18 (2009) 450–459.

[69] Y. Yano, A. Yamamoto, M. Ogura, K. Matsuzaki, Thermodynamics of insertion and self-association of a transmembrane helix: a lipophobic interaction by phosphatidylethanolamine, Biochemistry 50 (2011) 6806–6814.
[70] V. Anbazhagan, D. Schneider, The membrane environment modulates self-association of the human GpA TM domain–implications for membrane protein folding and transmembrane signaling, Biochim. Biophys. Acta 1798 (2010) 1899–1907.
[71] S. Mall, R. Broadbridge, R.P. Sharma, J.M. East, A.G. Lee, Self-association of model transmembrane alpha-helices is modulated by lipid structure, Biochemistry 40 (2001) 12379–12386.
[72] L. Cristian, J.D. Lear, W.F. DeGrado, Use of thiol-disulfide equilibria to measure the energetics of assembly of transmembrane helices in phospholipid bilayers, Proc. Natl. Acad. Sci. U. S. A. 100 (2003) 14772–14777.
[73] P. Lagüe, M.J. Zuckermann, B. Roux, Lipid-mediated interactions between intrinsic membrane proteins: dependence on protein size and lipid composition, Biophys. J. 81 (2001) 276–284.
[74] J. Tang, H. Yin, J. Qiu, M.J. Tucker, W.F. DeGrado, F. Gai, Using two fluorescent probes to dissect the binding, insertion, and dimerization kinetics of a model membrane peptide, J. Am. Chem. Soc. 131 (2009) 3816–3817.
[75] L. Janosi, A. Prakash, M. Doxastakis, Lipid-modulated sequence-specific association of glycophorin A in membranes, Biophys. J. 99 (2010) 284–292.
[76] G. Schreiber, G. Haran, H.X. Zhou, Fundamental aspects of protein–protein association kinetics, Chem. Rev. 109 (2009) 839–860.
[77] G.A. Caputo, R.I. Litvinov, W. Li, J.S. Bennett, W.F. Degrado, H. Yin, Computationally designed peptide inhibitors of protein–protein interactions in membranes, Biochemistry 47 (2008) 8600–8606.